THE EUROPEAN
PHYSICAL JOURNAL C

Explaining the $B^+ \to K^+ \nu\bar{\nu}$ excess via a massless dark photon

Emidio Gabrielli[1,2,3,a], **Luca Marzola**[3], **Kristjan Müürsepp**[3], **Martti Raidal**[3]

[1] Physics Department, University of Trieste, Strada Costiera 11, 34151 Trieste, Italy
[2] INFN, Sezione di Trieste, Via Valerio 2, 34127 Trieste, Italy
[3] NICPB, Rävala 10, 10143 Tallinn, Estonia

Abstract The Belle II collaboration has recently observed the rare decay $B^+ \to K^+ \nu\bar{\nu}$, finding an excess with respect to the Standard Model prediction. We explore the possibility that the data entails long-distance interactions induced by a massless dark photon, γ_D. This couples at the tree-level to an invisible, dark sector and to the Standard Model via higher-dimensional operators, such as the chromomagnetic-dipole coupling that we use to explain the excess. As the process $B^+ \to K^+ \gamma_D$ is forbidden by angular momentum conservation, the transition mediated by the off-shell dark photon yields a three-body final state comprising a pair of dark fermions that show as a missing energy continuum in the detector, faking the neutrino signature. We show that the Belle II data is explained for perturbative values of the parameters of the model. This scenario predicts new contributions to the neutral B meson decays $B^0 \to K^* \gamma_D$, in which the emission of a on-shell dark photon is allowed, yielding a monochromatic missing energy signature. Analogously, an excess due to the emission of a dark photon is predicted for the $B_s^0 \to \phi + E_{\rm miss}$ decay that could be scrutinized next at the LHCb experiments.

1 Introduction

The flavor changing neutral current (FCNC) processes showing in the B meson decays are a powerful tool for new physics (NP) searches. In particular, the semi-leptonic decays proceeding at the quark level through the $b \to s\nu\bar{\nu}$ transition offer an excellent arena to test the Standard Model (SM) predictions. Due to the absence of FCNC at the tree-level in the SM, these processes are also inherently sensitive to any NP interacting with quarks and leptons and, consequently, quite useful to constrain possible radiative effects sourced by heavy states beyond the SM.

Recently, the Belle II collaboration has measured the branching ratio (BR) related to the rare decay $B^+ \to K^+ \nu\bar{\nu}$ observed with a 3.5σ significance. The observation relied on two different strategies for measuring the BR: the standard hadronic-tag (had) method and the novel inclusive-tag (incl) technique. The branching ratios obtained are [1,2]

$$\mathrm{BR}(B^+ \to K^+ \nu\bar{\nu})_{\rm had} = \left(1.1^{+0.9+0.8}_{-0.8-0.5}\right) \times 10^{-5}, \quad (1.1)$$

$$\mathrm{BR}(B^+ \to K^+ \nu\bar{\nu})_{\rm incl} = (2.7 \pm 0.5 \pm 0.5) \times 10^{-5}, \quad (1.2)$$

where the quoted uncertainties correspond to the statistical and systematic errors, respectively. The combination of these measurements gives

$$\mathrm{BR}(B^+ \to K^+ \nu\bar{\nu})_{\rm exp} = (2.3 \pm 0.7) \times 10^{-5}, \quad (1.3)$$

to be compared with the corresponding SM prediction [3–6]

$$\mathrm{BR}(B^+ \to K^+ \nu\bar{\nu})_{\rm SM} = (4.29 \pm 0.23) \times 10^{-6}, \quad (1.4)$$

where the long-distance SM tree-level contribution from $B^+ \to \tau^+(\to K^+\bar{\nu})\nu$ was subtracted [5].

As we can see, the BR measurement (1.3) shows a 2.7σ discrepancy when compared with the SM prediction (1.4). The mismatch is driven by the inclusive-tag result and, since the hadronic-tag value is consistent with the SM expectation within errors, it could well be due to unknown uncertainties pertaining to the new method; future measurements will certainly clarify this issue.

In the meantime, one may wonder if the signal shows a preliminary hint of physics beyond the SM. In this case, the corresponding contribution to the BR indicated by the experiment is

$$\mathrm{BR}(B^+ \to K^+ \nu\bar{\nu})_{\rm NP} = (1.9 \pm 0.7) \times 10^{-5}. \quad (1.5)$$

The possible deviations of semi-leptonic B decays with neutrino final states from the SM predictions stem from two distinct classes of NP contributions. The first one, associated to the so called *indirect*-NP effects, is related to the presence of

[a] e-mail: emidio.gabrielli@cern.ch (corresponding author)

heavy NP particles that add to the SM Wilson coefficients of the interaction Hamiltonian describing the B semi-leptonic decays in the SM effective field theory approach. The other one is related to the so called *direct*-NP effects, and is linked to the presence of new invisible particles(antiparticles) $X(\bar{X})$ that could be produced via two-body $B^+ \to K^+ X$ or three-body $B^+ \to K^+ X \bar{X}$ decays, depending on the spin. When these particle are stable (or long-lived enough to escape the detector), they mimic the neutrino missing energy signature expected for $B^+ \to K^+ \nu \bar{\nu}$ within the SM. Several recent studies have suggested NP interpretations of the Belle II result, both in the framework of indirect [7–13] and direct NP effects [12,14–20].

In order to explain the Belle II result, we focus here on the latter possibility ascribing the excess to a pair of light dark fermions, Q_i, produced in the $B^+ \to K^+ Q_i \bar{Q}_i$ transition via long-distance interactions mediated by a massless dark photon γ_D. On general grounds, it is also expected that the same new FCNC interactions give contributions to the $B^0 \to K^*$ transition, which presently is consistent with the SM predictions for $B^0 \to K^* \nu \bar{\nu}$. Dark fermion production in B meson decays via short-distance interactions mediated by 4-fermions operators has been also considered in [21].

Massless dark photons are the quanta associated with an unbroken $U(1)_D$ gauge symmetry of a hypothetical dark sector, comprising particles that do not partake in the SM interactions. The dark photon scenario [22–26] has been extensively analyzed in the Literature, mainly in its massive limit, and is the subject of many current experimental searches [27] – see [28] for a recent review. Massless dark photons have been explored in the context of astrophysics and cosmology as sources of long range interactions ("dark electromagnetism") among the dark matter constituents [29–37]. Massless dark photons have also been employed to explain the SM flavor hierarchy puzzle [38,39] and the experimental tests of this scenario involving Higgs physics [40–47], flavor-changing neutral currents [48], kaon physics [49], and Z physics [50–52].

Unlike the massive case, a massless dark photon does not have tree-level interactions with ordinary matter and, for this reason, is much less constrained by experiments [25,28]. Contact with the SM is provided by effective couplings sourced at the loop level by heavy messenger fields, which connect the SM and the dark sector. For the SM fermions, the lowest-order coupling with the dark photon is provided by the magnetic-dipole operator [28,53] that could also induce FCNC transitions [48]. Hence, assuming that the dark sector comprises N_Q light dark fermions enjoying an unbroken $U(1)_D$ symmetry (a dark sector replica of QED), we study the inclusive decay $B^+ \to K^+ Q_i \bar{Q}_i$ due to the "dark" chromomagnetic-dipole operator for the $b \to s \gamma_D$ [48] process, including the relevant Sommerfeld-Fermi corrections [54]. The decay $B^+ \to K^+ \gamma_D$ is precluded by angular momentum conservation for a real massless dark photon. Consequently, the long-distance process underlying the transition must necessarily involve a virtual state yielding a dark fermion pair in the final state and the resulting $B^+ \to K^+ Q_i \bar{Q}_i$ decay can be used to explain the Belle II excess ascribed to $B^+ \to K^+ \nu \bar{\nu}$. Differently, the emission of a real dark photon is allowed in the related $B^0 \to K^* \gamma_D$ decay, which can be used to constrain the scenario since no events have been observed so far for this process. For the same reason, the scenario also entails the presence of a NP signal showing as $B_s^0 \to \phi + E_{\text{miss}}$ at dedicated searches and potentially observable already at the LHCb experiment.

The paper is organized as follows. In Sect. 2 we provide the theoretical framework describing the dark photon scenario and the relevant FCNC couplings. In Sects. 3 and 4 we provide analytical and numerical results for the branching ratios of $B^+ \to K^+ Q_i \bar{Q}_i$ and $B^0 \to K^* \gamma_D$, respectively. In Sect. 5 we analyze the Belle II excess and the constraints due to the $B^0 \to K^* \nu \bar{\nu}$ process. In Sect. 6, instead, we provide the predictions of the scenario for the $B_s^0 \to \phi \nu \bar{\nu}$ decay. Finally, our conclusions are given in Sect. 7.

2 Theoretical framework

In this section we analyze the Belle II excess within the framework of a NP scenario that leverages the phenomenology of dark photons.

Broadly speaking, dark photon models can be categorized into two distinct classes depending on whether the corresponding field quanta are massive or massless. The choice yields very different experimental signatures: a massless dark photon does not possess tree-level couplings to any SM current and is thus allowed to interact with ordinary matter only through operators of dimension higher than four [25,28,53]. Differently, massive dark photons can couple to ordinary matter via a renormalizable operator of dimension four involving an arbitrarily small charge [25]. The two classes are disjoint, in that the massless case cannot be obtained as a limiting case of massive dark photon models. For the sake of explaining the Belle II excess, we will resort to a massless dark photon.

In order to describe the FCNC interactions causing the $b \to s$ transition of interest, we use the following effective Lagrangian involving b and s quarks

$$\mathcal{L}_{eff} = \frac{1}{2\Lambda} \left[\bar{s} \sigma_{\mu\nu} b \right] F_D^{\mu\nu} + h.c. , \qquad (2.1)$$

where $\sigma_{\mu\nu} = i/2 [\gamma_\mu, \gamma_\nu]$, and the $F_D^{\mu\nu} = \partial^\mu A_D^\nu - \partial^\nu A_D^\mu$ is the dark photon field strength tensor. The effective scale Λ depends on the couplings and masses of the dark and messenger sectors as specified in Ref. [48]. In addition, we assume

that the dark photon is coupled to dark fermions in a way reminiscent of QED within the SM,

$$\mathcal{L}_{dark} = e_D \sum_i q_i \left[\bar{Q}_i \gamma_\mu Q_i \right] A_D^\mu, \tag{2.2}$$

where the index i indicates the dark fermion generation, e_D is the coupling of the $U(1)_D$ group with the corresponding dark fine-structure constant $\alpha_D = e_D^2/4\pi$, and q_i are the corresponding charges of the dark fermions Q_i.

3 Decay width for $B^+ \to K^+ Q\bar{Q}$

Consider now the B^+ meson decay

$$B^+(p_B) \to K^+(p_K) \; Q(k_1) \bar{Q}(k_2), \tag{3.1}$$

where p_B, p_K, and $k_{1,2}$ are four-momenta and Q stands for a generic dark-fermion Q_i. For simplicity we assume all dark fermions have unit charge $q_i = 1$.[1]

Using the interaction Lagrangian terms in Eq. (2.1) and Eq. (2.2), the corresponding decay amplitude is given by

$$\mathcal{M} = \frac{-ie_D}{\Lambda} \langle K | [\bar{s}\sigma_{\mu\nu}b] | B \rangle \frac{q^\nu}{s} \left[\bar{Q}\gamma^\mu Q \right], \tag{3.2}$$

where $s = q^2$ and $q^\mu = k_1 + k_2$ is the off-shell dark photon momentum. In order to simplify the notation, in the following we often leave the charge specification for the B^+ and K^+ mesons understood.

For the tensor hadronic matrix element $\langle K | \bar{s}\sigma_{\mu\nu}b | B \rangle$, we use the parametrization provided in Ref. [55], obtaining

$$\langle K(p_K) | \left[\bar{s}\sigma_{\mu\nu}q^\nu b \right] | B(p_B) \rangle$$
$$= i \left[(p_B + p_K)_\mu s - q_\mu (m_B^2 - m_K^2) \right] \frac{f_T(s)}{m_B + m_K}, \tag{3.3}$$

where the form factor $f_T(s)$ was computed in Ref. [56] by using the light cone sum rule (LCSR) approach. Its expression, as a function of s, is given by

$$f_T(s) = \frac{f_T(0)}{1 - s/m_{\mathrm{res,T}}^2}$$
$$\times \left\{ 1 + b_1^T \left[z(s) - z(0) + \frac{1}{2} \left(z(s)^2 - z(0)^2 \right) \right] \right\}, \tag{3.4}$$

with

$$z(s) = \frac{\sqrt{\tau_+ - s} - \sqrt{\tau_+ - \tau_0}}{\sqrt{\tau_+ - s} + \sqrt{\tau_+ - \tau_0}},$$
$$\tau_0 = \sqrt{\tau_+} \left(\sqrt{\tau_+} - \sqrt{\tau_+ - \tau_-} \right), \quad \tau_\pm = (m_B \pm m_K)^2. \tag{3.5}$$

The values of the b_1^T and $f_T(0)$ coefficients, as well as of the resonance mass $m_{\mathrm{res,T}}$, can be found in Ref [56]. Then, following the notation of Ref. [55], the differential decay width $d\Gamma/d\hat{s}$ for the process $B \to K Q_i \bar{Q}_i$ is found to be

$$\frac{d\Gamma^K}{d\hat{s}} = \frac{\alpha_D m_B^5}{32\pi^2 m_b^2 \Lambda^2} \bar{u}(\hat{s}) \left(\lambda(\hat{s}) - \frac{\bar{u}(\hat{s})^2}{3} \right)$$
$$\times \frac{\hat{m}_b^2}{(1 + \hat{m}_K)^2} |f_T(s)|^2, \tag{3.6}$$

where $\hat{s} = s/m_B^2$, $\hat{m}_b = m_b/m_B$, $\hat{m}_K = m_K/m_B$, with m_b the b quark pole mass, and m_B and m_K the B^+ and K^+ masses respectively. The functions $\lambda(\hat{s})$ and $\bar{u}(\hat{s})$ are defined as

$$\bar{u}(\hat{s}) = \sqrt{\lambda(\hat{s}) \left(1 - 4\frac{\hat{m}_Q^2}{\hat{s}} \right)}, \tag{3.7}$$
$$\lambda(\hat{s}) = 1 + \hat{m}_K^4 + \hat{s}^2 - 2\hat{s} - 2\hat{m}_K^2 (1 + \hat{s}),$$

where $\hat{m}_Q = m_Q/m_B$, and m_Q is the dark fermion mass.

By integrating the differential width in Eq. (3.6) over the kinematic range of $\hat{s}$,

$$4\hat{m}_Q^2 \leq \hat{s} \leq (1 - \hat{m}_K)^2, \tag{3.8}$$

and dividing by the B^+ total width, we obtain the following value for the relevant BR,

$$\mathrm{BR}(B^+ \to K^+ Q\bar{Q}) \simeq 5.43 \times 10^{-6} \left(\frac{10^5 \mathrm{TeV}}{\Lambda} \right)^2 \alpha_D \tag{3.9}$$

valid for $\hat{m}_Q \simeq 0$. For comparison, the SM result for the differential width is given by [4]

$$\frac{d\Gamma_{\mathrm{SM}}^K}{d\hat{s}} (B^+ \to K^+ \nu\bar{\nu})$$
$$= \frac{G_F^2 m_B^5 \alpha_{EW}^2 |V_{tb} V_{ts}^*|^2 X_t^2}{16^2 \pi^5 \sin^4 \theta_W} |f_+(s)|^2 \lambda^{3/2}(\hat{s}), \tag{3.10}$$

where $X_t \simeq 1.462$ (including the NLO QCD corrections [57–59] and two-loop EW contributions [60]) V_{tb} and V_{ts} are the CKM matrix elements, θ_W the Weinberg angle and α_{EW} the QED fine structure constant evaluated at the top-quark mass scale. For the input parameters in Eq. (3.10) we use the central values [4] $\alpha_{EW}^{-1} = 127.925$, $\sin^2 \theta_W = 0.23126$, $|V_{tb} V_{ts}^*| = 0.0401$. The form factor $f_+(s)$ is computed in LCSR approach [56] and is related to the matrix element of the vector operator as

$$\langle K(p_K) | \left[\bar{s}\gamma_\mu b \right] | B(p_B) \rangle$$
$$= f_+(s) \left[(p_B + p_K)_\mu - \frac{m_B^2 - m_K^2}{s} q_\mu \right]$$
$$+ \frac{m_B^2 - m_K^2}{s} f_0(s) q_\mu. \tag{3.11}$$

---

[1] This setup serves to approximate more general scenarios where different generations of dark fermions have charges of the same order of magnitude: the overall coupling strength can be reabsorbed in the definition of α_D.

Its expression is given by [56]

$$
f_+(s) = \frac{f_+(0)}{1 - s/m_{\text{res},+}^2}
$$

$$
\times \left\{ 1 + b_1^+ \left[z(s) - z(0) + \frac{1}{2} \left(z(s)^2 - z(0)^2 \right) \right] \right\}, \quad (3.12)
$$

where the values for the coefficients b_1^+ and resonant mass $m_{\text{res},+}$ can be found in Ref. [56]. Notice that, for vanishing dark fermion masses, the q^2 distributions in Eq. (3.6) tend to the SM contribution modulo an overall multiplying factor.

3.1 Sommerfeld-Fermi and dark magnetic-dipole corrections

The Sommerfeld-Fermi enhancement (SF) [61,62] is a long-distance correction to the amplitude in Eq. (3.6) relevant for the large values of α_D required to explain the excess. The re-summation of the leading log terms induced, in this case, by the soft photon-like corrections, is equivalent to the inclusion of the Coulomb interaction in the wave function of final states [63]. In our case, the contribution is particularly important in a kinematic regime where the final charged particles are non-relativistic in the rest frame of the decaying B meson.

The SF correction can be accounted for in the computation of the differential branching ratio by including the corresponding overall enhancement factor [54]

$$
d\Gamma_{\text{SF}}^K = \Omega(\beta_{12}) \, d\Gamma^K,
$$

$$
\Omega(\beta_{12}) = \frac{2\pi \alpha_D q_i^2}{\beta_{12}} \frac{1}{1 - \exp\left[-\frac{2\pi \alpha_D q_i^2}{\beta_{12}} \right]}, \quad (3.13)
$$

where $d\Gamma^K$ is given in Eq. (3.6) and

$$
\beta_{12} = \sqrt{1 - \frac{m_Q^4}{(s - 2m_Q^2)^2}}, \quad (3.14)
$$

with q_i being the $U(1)_D$ charge of the dark fermion of the generation i (that we set to unity in our analysis). For scenarios with large values of $\alpha_D \simeq \mathcal{O}(1)$, the SF provides large contributions also in the q^2 region away from the dark fermion production threshold. Furthermore, in the presence of this correction, the dependence of the differential BR on α_D is more involved than in Eq. (3.6), where the parameters simply gives an overall multiplying factor.

The effect of SF corrections is shown in Fig. 1, where we plot the dependence of the relevant differential BR on q^2 for three generations of dark fermions and different values of the NP parameters, including (solid lines) and omitting (dashed lines) the SF enhancement. The SM result, included for reference, is shown in black. As we can see, the effect of the SF correction is quite large: over the relevant kinematic region, the SF correction results in an enhancement of the

differential BR by a factor of about 5 for the examined cases of $\alpha_D = 0.7$ and $\alpha_D = 1.0$.

Besides the SF enhancement we scrutinize also the impact of radiative corrections sourced by the dark $U(1)$ interaction. As the SM particles do not partake in it, the corrections affect only the diagram involving dark fermions. These include, at the one-loop level, the dark photon – dark fermion vertex and the self-energy diagram of the latter. Since we are interested in long-distance effects, we retain only the $\mathcal{O}(\alpha_D)$ dark magnetic-dipole corrections affecting the F_2 form factor – which multiplies the $\sigma_{\mu\nu}$ operator in the dark fermion effective vertex. The correction is relevant for large values of α_D in the q^2 region close to the kinematic threshold and can be included in the computation by replacing the function $\lambda(\hat{s})$ in Eq. (3.6) with

$$
\lambda(\hat{s}) \to \lambda(\hat{s}) \left[1 + \Delta_M(\hat{s}) \right], \quad (3.15)
$$

where the correction $\Delta_M(\hat{s})$ is given by [64]

$$
\Delta_M(\hat{s}) = 4\hat{m}_Q \, \text{Re}\left[F_2(\hat{s}) \right] + \frac{1}{3} \left| F_2(\hat{s}) \right|^2 \left(\hat{s} + 8\hat{m}_Q^2 \right), \quad (3.16)
$$

and the magnetic form factor $F_2(\hat{s})$ is

$$
F_2(\hat{s}) = \frac{\alpha_D}{2\pi} \frac{\hat{m}_Q}{\sqrt{\hat{s}(\hat{s} - 4\hat{m}_Q^2)}}
$$

$$
\times \log\left[\frac{2\hat{m}_Q^2 - \hat{s} + \sqrt{\hat{s}(\hat{s} - 4\hat{m}_Q^2)}}{2\hat{m}_Q^2} \right], \quad (3.17)
$$

with log the logarithm in the natural basis. Differently from the case of the SF correction, we find that the integrated effect of the magnetic-dipole correction on the q^2 region relevant for the Belle II excess, being at the percent level, is negligible.

4 Decay width for $B^0 \to K^* \gamma_D$

As mentioned in the introduction, the presence of a dark photon can also affect other decay processes involving the $b \to s$ FCNC transition. In particular, angular momentum conservation allows the emission of an on-shell massless dark photon in the following decay of the B^0 neutral meson

$$
B^0(p_B) \to K^*(p_K) \, \gamma_D(q), \quad (4.1)
$$

where p_B, p_K, and q indicate the involved four momenta. The process, which proceeds analogously to the $B^0 \to K^* \gamma$ decay in the SM, is induced by the interaction Lagrangian in Eq. (2.1) used to model the decay in Eq. (3.1).

The matrix element for this transition is given by

$$
\mathcal{M} = \frac{-i e_D}{\Lambda} \langle K^* | \left[\bar{s} \sigma_{\mu\nu} q^\nu b \right] | B^0 \rangle \varepsilon_D^\mu(q), \quad (4.2)
$$

Fig. 1 Differential BR for the process $B^+ \to K^+ Q\bar{Q}$ as a function of the missing energy q^2, for $N_Q = 3$ generations of dark fermions all with mass $m_Q = 0.5$ GeV. The dashed lines use the expression in Eq. (3.6), whereas the solid lines include the SF correction, Eq. (3.13). The SM result, in Eq. (3.10), is shown in black
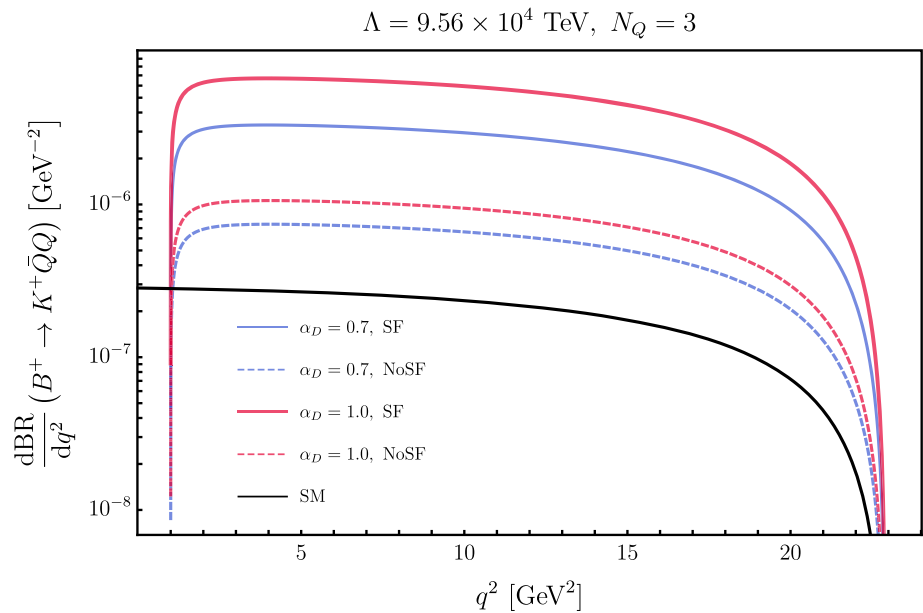
where $\varepsilon_D^\mu(q)$ is the dark photon polarization vector. For the tensor hadronic matrix element $\langle K^* | \bar{s}\sigma_{\mu\nu} b | B^0 \rangle$ we use again the parametrization provided in Ref. [55], which in the general case of $q^2 \neq 0$ gives

$$\langle K^*(p_K) | [\bar{s}\sigma_{\mu\nu} q^\nu b] | B^0(p_B) \rangle = i2\epsilon_{\mu\nu\alpha\beta} \, \varepsilon^{\dagger\nu} p_B^\alpha p_K^\beta T_1(s)$$
$$+ T_2(s) \left[\varepsilon_\mu^\dagger \left(m_B^2 - m_{K^*}^2 \right) - \left(\varepsilon^\dagger \cdot p_B \right) (p_B + p_K)_\mu \right]$$
$$+ T_3(s) \left(\varepsilon^\dagger \cdot p_B \right) \left[q_\mu - \frac{s}{m_B^2 - m_{K^*}^2} (p_B + p_K)_\mu \right],$$

$$(4.3)$$

where ε and m_{K^*} are the polarization vector and mass of the K^* meson, respectively, and m_B is the B^0 mass. The terms $T_{1,2,3}(s)$ are form factors and the convention $\epsilon_{0123} = +1$ is used for the Levi-Civita symbol. Only the $T_1(s)$ form factor contributes to the matrix element of Eq. (4.3) for the operator $[\bar{s}\sigma_{\mu\nu}q^\nu b]$, while $T_{2,3}(s) = 0$ due to parity.

By combining the effective Lagrangian in Eq. (2.1) with the hadronic matrix elements in Eq. (4.3), we obtain for the corresponding decay width [64]

$$\Gamma(B^0 \to K^*\gamma_D) = \frac{m_B^3 |T_1(0)|^2 \left(1 - \hat{m}_{K^*}^2 \right)^3}{32\pi \Lambda^2}, \quad (4.4)$$

where $\hat{m}_{K^*} = m_{K^*}/m_B$ and $T_1(0) \simeq 0.28$ [56] is the hadronic form factor evaluated at $s = 0$ and defined in Eq. (4.3).

Finally, the BR of the process under scrutiny then is

$$\text{BR}(B^0 \to K^*\gamma_D) = 2.47 \times 10^{-5} \left(\frac{10^5 \text{TeV}}{\Lambda} \right)^2. \quad (4.5)$$

Present searches from the BaBar [65] and Belle [66] collaborations have only set upper bounds on the $\text{BR}(B^0 \to K^* \nu\bar{\nu})$ which is compatible with the SM expectations [3]. In

particular, the most recent result by the Belle collaboration is $\text{BR}(B^0 \to K^*\nu\bar{\nu}) < 2.7 \times 10^{-5}$ at 90% C.L. [66]. The invisible $\nu\bar{\nu}$ system shows as continuous missing energy E_{miss} distribution in the detector and a kinematic cut $E_{\text{miss}} > 2.5\,\text{GeV}$, in the B^0 meson rest frame, has been used in the analysis.

It could be thought that the upper bound on $\text{BR}(B^0 \to K^*\nu\bar{\nu})$ may be used to constrain also the $B^0 \to K^*\gamma_D$ decay. However, the experimental signatures of the two processes differ in that the final state possesses different kinematic properties. In more detail, the two-body decay $B^0 \to K^*\gamma_D$ yields a monochromatic missing energy distribution set at the specific value $E_{\gamma_D} = E_{\text{miss}} = 2.56\,\text{GeV}$ in the B^0 rest frame. As mentioned before, three bodies decays such as $B^0 \to K^*\nu\bar{\nu}$ result instead in a continuous E_{miss} distribution. For this reason, strictly speaking, applying the limits in Ref. [66] to the $\text{BR}(B^0 \to K^* \gamma_D)$ is not completely correct and a dedicated analysis would be required to set limits on the process [67]. Bearing this caveat in mind, in the following we will still assume that the Belle upper bound on the $\text{BR}(B^0 \to K^*\nu\bar{\nu})$ [66] holds true also for the $B^0 \to K^*\gamma_D$ decay and analyze its phenomenological implications within the present context. We remark that this constraint is comparable to the limit $\text{BR}(B^0 \to K^*\nu\bar{\nu}) < 5.3 \times 10^{-5}$ obtained in Ref. [68] by recasting the BaBar result [65] for searches involving a light axion in place of the dark photon.

Imposing the experimental upper limit on $\text{BR}(B^0 \to K^*\nu\bar{\nu}) < 2.7 \times 10^{-5}$ gives a lower bound,

$$\Lambda \geq 9.56 \times 10^4 \text{ TeV}, \quad (4.6)$$

that is about 32 times stronger than the one obtained from the inclusive decay $\text{BR}(b \to s X_{\text{inv}}) < \mathcal{O}(10\%)$ [69]. Notice that bounds from $B^0 - \bar{B}^0$ oscillations [21] do not constrain the effective scale Λ entering the $b \to s\gamma_D$ transition: the box diagrams involved in the oscillation do not depend on

the couplings responsible for generating the scale Λ in the UV completion of the theory. We also remark that the bound in Eq. (4.6) allows the framework to satisfy also the NP constraint due to the $B \to X_s \gamma$ decay at 95% C.L. even when large values of α_D are considered [64]. The relevance of this latter bound, however, strongly depends on the UV completion of the theory describing the emergence of the effective scale Λ. Finally, we would like to stress that also the constraints from the $B_s^0 \to$ invisible decay, implemented here by the $B_s^0 \to Q_i \bar{Q}_i$ process, do not apply. Indeed, the magnetic dipole interaction vertex in Eq. (2.1), allowing the $B_s^0 \to Q_i \bar{Q}_i$ decay, yields a contribution that identically vanishes since $\langle 0 | [\bar{s} \sigma_{\mu\nu} q^\nu b] | B_s^0(q) \rangle = 0$.

5 Fitting the $B^+ \to K^+ \nu \bar{\nu}$ excess

Here we consider the impact of the massless dark photon scenario on the present 2.7σ discrepancy in Eq. (1.4) with respect to the SM prediction for the BR of $B^+ \to K^+ \nu \bar{\nu}$ decay. As discussed in the introduction, we assume here that the difference due to NP effects in Eq. (1.5) with the missing energy is carried away by the dark fermion in place of SM neutrinos.

In order to simplify the analysis, we fit the excess in Eq. (1.5) assuming the production of N_Q generations of dark-fermions all with unit charge and consider the inclusive dark fermion decay defined as $\mathrm{BR}(B^+ \to K^+ Q_X \bar{Q}_X) = \sum_{i=1}^{N_Q} \left[\mathrm{BR}(B^+ \to K^+ Q_i \bar{Q}_i) \right]$. Accounting for the constraint discussed in the previous section and for the SF correction we have

$$\frac{\mathrm{BR}(B^0 \to K^* \gamma_D)}{\mathrm{BR}(B^+ \to K^+ Q_X \bar{Q}_X)_{\mathrm{SF}}} \simeq \frac{0.72}{N_Q} \quad \text{for } \alpha_D \sim \mathcal{O}(1),$$

(5.1)

and imposing $\mathrm{BR}(B^+ \to K^+ Q_X \bar{Q}_X) = \mathrm{BR}(B^+ \to K^+ + \mathrm{inv})_{\mathrm{NP}} \sim 1.9 \times 10^{-5}$ from Eq. (1.5), then gives

$$\mathrm{BR}(B^0 \to K^* \gamma_D) \simeq \frac{1.37}{N_Q} \times 10^{-5}.$$

(5.2)

Since no excess has been observed for the $B^0 \to K^* \nu \bar{\nu}$ transition, applying the upper bound on $\mathrm{BR}(B^0 \to K^* \nu \bar{\nu}) < 2.7 \times 10^{-5}$ to the $\mathrm{BR}(B^0 \to K^* \gamma_D)$ we obtain

$$N_Q \geq 1,$$

(5.3)

for the number of dark fermion generations. Equation (5.3) then shows that a strong (but still perturbative) dark photon coupling to the dark sector, $\alpha_D \sim \mathcal{O}(1)$, allows to explain the excess in the decay $\mathrm{BR}(B^+ \to K^+ \nu \bar{\nu})$ through the incoherent production of N_Q light dark fermions.

In Fig. 2 we show the parameter values for which our scenario can reproduce the Belle II excess through Eq. (3.13).

The yellow horizontal band in the top panel shows the 1σ confidence interval identified by the experiment. The colored lines show the solutions of the model for the indicated values of the dark fermion masses, assuming three generations of particles degenerate in mass. As we can see, the anomaly can be matched for perturbative values of the (universal) dark fine-structure constant α_D. In the plot we used the value of the effective scale Λ saturating the lower bound in Eq. (4.6). The bottom panel shows instead the value of the BR relevant to reproduce the excess as a function of the same scale and α_D for a benchmark value of the dark fermion mass, $m_Q = 0.5$ GeV, shared by three generations of particles. The constraint in Eq. (4.6) excludes the area below the black dashed line.

The relation that the scenario establishes between the decays $B^0 \to K^* \gamma_D$ and $B^+ \to K^+ Q_X \bar{Q}_X$ is explored in Fig. 3. The solid lines show the ratio of the corresponding BRs as a function of α_D, obtained for $N_Q = 3$ generation of dark fermions sharing the indicated mass values. Importantly, the dependence of the BRs on the effective scale Λ drops out in the ratio. The red dashed line shows the value supported by the NP interpretation of the Belle II excess, Eq. (1.5), once the upper bound $\mathrm{BR}(B^0 \to K^* \nu \bar{\nu}) < 2.7 \times 10^{-5}$ is assumed. The latter excludes the solutions falling in the area dashed in red. Future measurements of $\mathrm{BR}(B^0 \to K^* \nu \bar{\nu})$ can be used to constrain the value of the dark fine-structure constant α_D and a simultaneous fit of the Belle II excess would then allow the determination of the effective scale Λ.

6 Predicting a possible signal in B_s^0 decays

In the previous section we have shown that the Belle II excess in $B^+ \to K^+ \nu \bar{\nu}$ can be explained by the production of dark fermion pairs in the process $B^+ \to K^+ Q_i \bar{Q}_i$, mediated by a massless off-shell dark photon. In order to test this interpretation of the Belle II data, we seek further phenomenological consequences of the same interaction Lagrangian (2.1) used to model the excess.

The magnetic-dipole operator in Eq. (2.1) for the $b \to s$ transition can also contribute to the $B_s^0 \to \phi \nu \bar{\nu}$ decay, thereby inducing an excess over the SM predictions for $B_s^0 \to \phi \nu \bar{\nu}$ [70]

$$\mathrm{BR}(B_s^0 \to \phi \nu \bar{\nu})_{\mathrm{SM}} = (1.4 \pm 0.4) \times 10^{-5}.$$

(6.1)

The process $B_s^0 \to \phi \gamma_D$ shows in experiments as $B_s^0 \to \phi + \mathrm{E_{miss}}$ with the massless dark photon carrying away an energy $E_{\mathrm{miss}} = 2.59$ GeV in the B_s^0 rest frame, in complete analogy with the $B^0 \to K^* \gamma_D$ transition. The present upper limit on this BR comes from LEP data and is given by [71]

$$\mathrm{BR}(B_s^0 \to \phi \nu \bar{\nu})_{\mathrm{exp}} < 5.4 \times 10^{-3}$$

(6.2)

at 90% confidence level.

Fig. 2 Values of the parameters for which the scenario can explain the Belle II excess through the BR given by Eq. (3.13). The top panel shows three different solutions obtained by varying the mass value shared by three generation of dark fermions for the value of the effective scale Λ indicated by Eq. (4.6). The bottom panel shows the dependence on the effective scale and dark fine-structure constant α_D of the BR obtained by integrating Eq. (3.13)
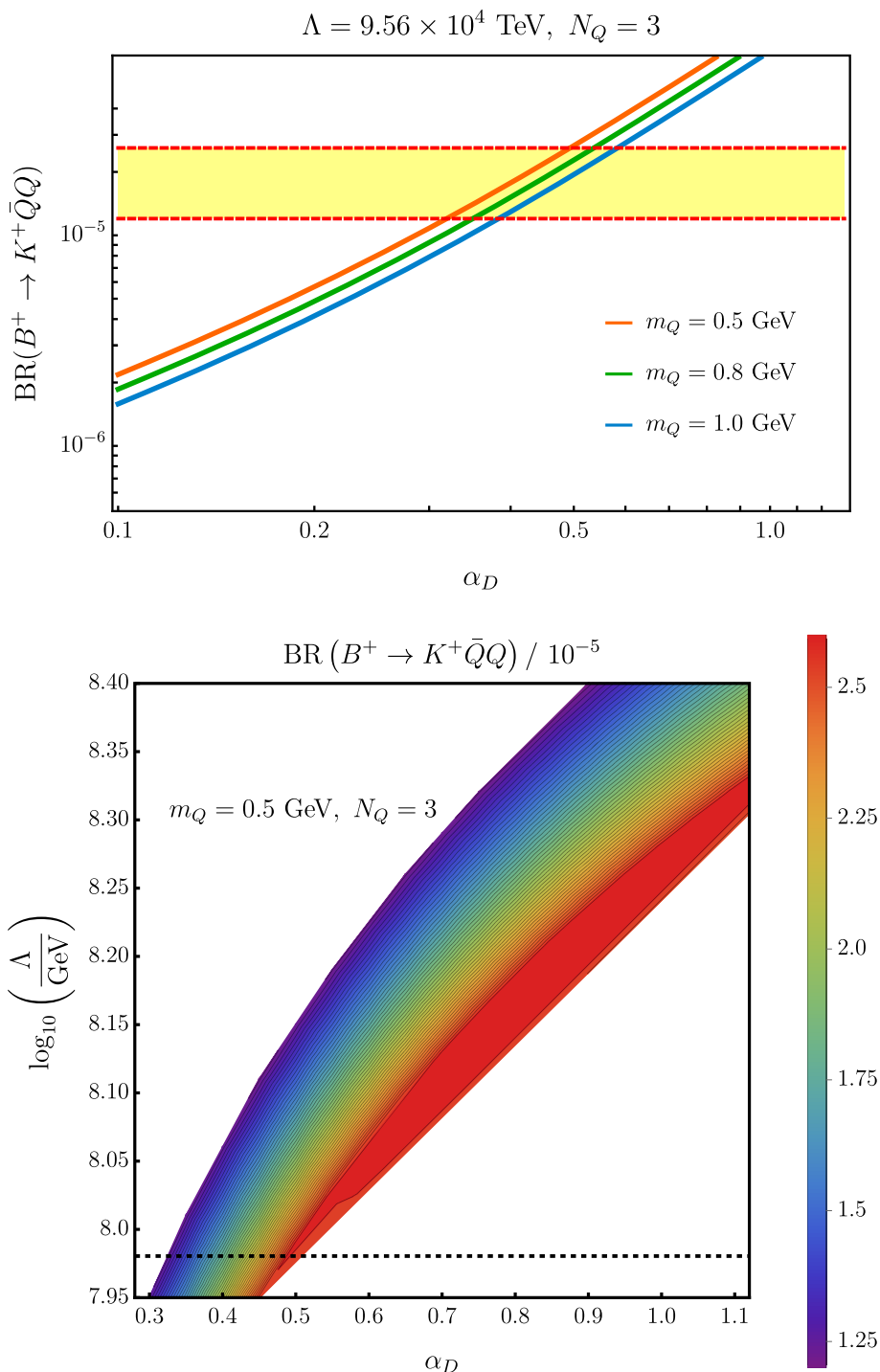

The prediction of the scenario for the $\mathrm{BR}(B_s^0 \to \phi\gamma_D)$ can be obtained by noticing that the transition depends on the same hadronic matrix element (the magnetic dipole operator $\langle\phi|[s\sigma_{\mu\nu}b]|B_s^0\rangle$) that enters the $B_s^0 \to \phi\gamma$ decay. The same holds true for the matrix element $\langle K^*|[s\sigma_{\mu\nu}b]|B^0\rangle$, which enters both the $\mathrm{BR}(B^0 \to K^*\gamma_D)$ and $\mathrm{BR}(B^0 \to K^*\gamma)$. The ratio measured at LHCb [72]

$$R_{K^*\phi} = \frac{\mathrm{BR}(B^0 \to K^*\gamma)}{\mathrm{BR}(B_s^0 \to \phi\gamma)} = 1.23\,(6)_{\mathrm{stat}}\,(4)_{\mathrm{syst}}\,(10)_{f_s/f_d}, \quad (6.3)$$

where the third uncertainty is associated with the ratio of fragmentation fractions f_s/f_d, allows us to infer the hadronic tensor form factor $T_1^{B_s^0 \to \phi}$ for the $\mathrm{BR}(B_s^0 \to \phi\gamma_D)$ – or, analogously, for the $\mathrm{BR}(B_s^0 \to \phi\gamma)$ – from the corresponding tensor form factor $T_1^{B^0 \to K^*}$ of $\mathrm{BR}(B^0 \to K^*\gamma_D)$ in Eq. (4.3) evaluated at $s = 0$. In particular, Ref. [73] gives

$$R_{K^*\phi} = |r_{K^*\phi}|^2 C_{K^*\phi}\,(1 + \delta_{WA})\,, \quad (6.4)$$

Fig. 3 Dependence of $\mathrm{BR}(B^0 \to K^*\gamma_D)/\mathrm{BR}(B^+ \to K^+ Q_X \bar{Q}_X)$ on the dark fine-structure constant α_D. The ratio is for $N_Q = 3$ generations of dark fermions sharing the indicated mass values and does not depend on the effective scale Λ. The dashed red line indicates the value obtained for the NP interpretation of the Belle II excess, Eq. (1.5), assuming the current experimental bound $\mathrm{BR}(B^0 \to K^*\nu\bar{\nu}) < 2.7 \times 10^{-5}$. The latter excludes solution falling in the area hatched in red. Future determinations of $\mathrm{BR}(B^0 \to K^*\nu\bar{\nu})$ can be used to constrain the parameter space of the model as described in the text
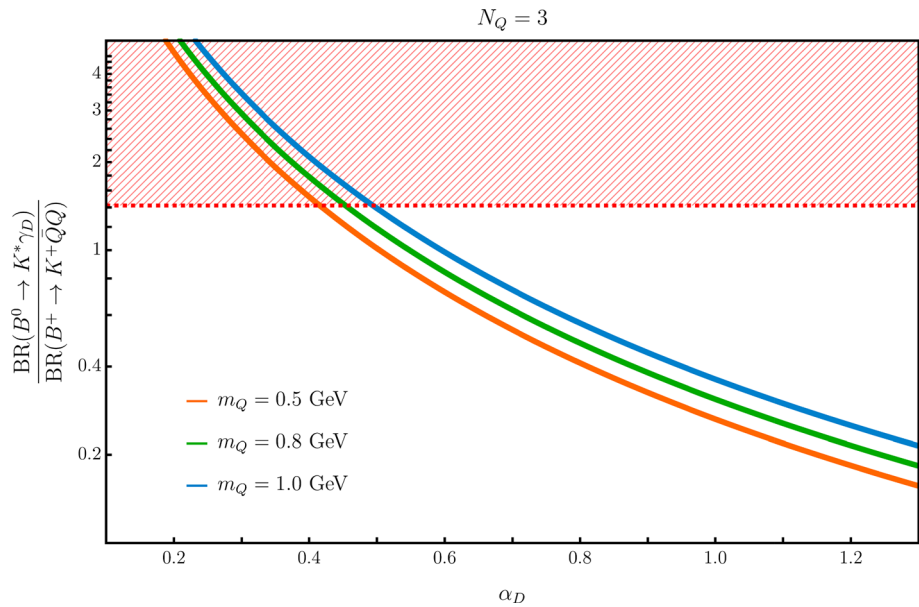
where the term $\delta_{WA} \simeq 0.02$ contains weak interaction corrections,

$$r_{K^*\phi} = \frac{T_1^{B^0 \to K^*}}{T_1^{B_s^0 \to \phi}}, \tag{6.5}$$

and

$$C_{K^*\phi} = \frac{\tau_{B^0}}{\tau_{B_s^0}} \left(\frac{m_B}{m_{B_s}}\right)^3 \left(\frac{1 - m_{K^*}^2/m_B^2}{1 - m_\phi^2/m_{B_s}^2}\right)^3 = 1.01. \tag{6.6}$$

Since δ_{WA} is negligible, we approximate $R_{K^*\phi} \simeq r_{K^*\phi}^2$ and with the central value from Eq. (6.4) extract $r_{K^*\phi}$ to predict the $\mathrm{BR}(B_s^0 \to \phi\gamma_D)$ to be

$$\mathrm{BR}(B_s^0 \to \phi\gamma_D) = 4.02 \times 10^{-5} \left(\frac{10^5 \mathrm{TeV}}{\Lambda}\right)^2. \tag{6.7}$$

Finally, by using the value of the scale Λ saturating the lower bound in Eq. (4.6) we obtain

$$\mathrm{BR}(B_s^0 \to \phi\gamma_D) \lesssim 2 \times 10^{-5}, \tag{6.8}$$

in agreement with the current constraint (6.2) from LEP searches. Importantly, the upper bound could fall within the sensitivity of future LHCb searches, as well as within the reach of future collider experiments running at the Z-pole [74,75].

7 Conclusions

We have shown that the recent measurement of $\mathrm{BR}(B^+ \to K^+\nu\bar{\nu})$ by the Belle II Collaboration, yielding a 2.7σ discrepancy with respect to the SM prediction, can be explained by dark fermion pair production through the process $B^+ \to K^+ Q_i \bar{Q}_i$ mediated by an off-shell massless dark photon.

The excess can be fitted with dark fermion masses of the order of 500 MeV, which experimentally result in a missing energy signature. The absence of the two body decay $B^+ \to K^+\gamma_D$ is ensured, for a massless dark photon, by the angular momentum conservation.

Since a dark photon emission is allowed in the $B^0 \to K^*\gamma_D$ transition, the lack of an observed signal related to the $B^0 \to K^*\nu\bar{\nu}$ decay gives $N_Q \gtrsim 1$ for $\alpha_D \sim \mathcal{O}(1)$. In regard of this, large but perturbative values of α_D are still experimentally viable for a massless dark photon, as the scenario is only loosely constrained due to the naturally suppressed couplings with the visible sector. We also remark that the bound for the $B^0 \to K^*\nu\bar{\nu}$ process cannot be straightforwardly taken at face value to constrain the scenario via the related $B^0 \to K^*\gamma_D$ due to differences in the kinematics of the involved final states.

If the proposed dark fermion production mechanism is responsible for the Belle II excess, we predict the appearance of NP signals in the $B_s^0 \to \phi\gamma_D$ decay (and in $B^0 \to K^*\gamma_D$, should the aforementioned bound not hold), which could be scrutinized at the next LHCb experiment. These searches are crucial to test the massless dark photon interpretation of the Belle II excess in $B^+ \to K^+\nu\bar{\nu}$ decays. The expected phenomenological signature, in both channels, is a monochromatic missing energy distribution centered at the value $E_{\mathrm{miss}} = 2.56\,\mathrm{GeV}$ and $E_{\mathrm{miss}} = 2.59\,\mathrm{GeV}$ in the B meson rest frame, for the $B^0 \to K^*\gamma_D$ and $B_s^0 \to \phi\gamma_D$ transitions, respectively. We urge the experimental collaborations to start dedicated analysis targeted at these decay modes.

References

1. Belle-II Collaboration, E. Ganiev, Parallel talk given at the EPS-HEP2023 Conference in Hamburg (Germany, Aug 20–25, 2023). https://indico.desy.de/event/34916/contributions/146877/

2. Belle-II Collaboration, I. Adachi et al., Evidence for $B^+ \to K^+ \nu \bar{\nu}$ decays. arXiv:2311.14647

3. W. Altmannshofer, A.J. Buras, D.M. Straub, M. Wick, New strategies for New Physics search in $B \to K^* \nu \bar{\nu}$, $B \to K \nu \bar{\nu}$ and $B \to X_s \nu \bar{\nu}$ decays. JHEP **04**, 022 (2009). arXiv:0902.0160

4. A.J. Buras, J. Girrbach-Noe, C. Niehoff, D.M. Straub, $B \to K^{(*)} \nu \bar{\nu}$ decays in the Standard Model and beyond. JHEP **02**, 184 (2015). arXiv:1409.4557

5. HPQCD Collaboration, W.G. Parrott, C. Bouchard, C.T.H. Davies, Standard Model predictions for $B \to K \ell + \ell-$, $B \to K \ell 1 - \ell 2 +$ and $B \to K \nu \nu^-$ using form factors from Nf=2+1+1 lattice QCD. Phys. Rev. D **107**(1), 014511 (2023). arXiv:2207.13371. [Erratum: Phys. Rev. D 107, 119903 (2023)]

6. D. Bečirević, G. Piazza, O. Sumensari, Revisiting $B \to K^{(*)} \nu \bar{\nu}$ decays in the Standard Model and beyond. Eur. Phys. J. C **83**, 3 252 (2023). arXiv:2301.06990

7. P. Athron, R. Martinez, C. Sierra, B meson anomalies and large $B^+ \to K^+ \nu \bar{\nu}$ in non-universal $U(1)'$ models. arXiv:2308.13426

8. R. Bause, H. Gisbert, G. Hiller, Implications of an enhanced $B \to K \nu \bar{\nu}$ branching ratio. arXiv:2309.00075

9. L. Allwicher, D. Becirevic, G. Piazza, S. Rosauro-Alcaraz, O. Sumensari, Understanding the first measurement of $B(B \to K \nu \nu^-)$. Phys. Lett. B **848**, 138411 (2024). arXiv:2309.02246

10. X.-G. He, X.-D. Ma, G. Valencia, Revisiting models that enhance $B^+ \to K^+ \nu \bar{\nu}$ in light of the new Belle II measurement. arXiv:2309.12741

11. A. Datta, D. Marfatia, L. Mukherjee, $B \to K \nu \bar{\nu}$, MiniBooNE and muon $g - 2$ anomalies from a dark sector. arXiv:2310.15136

12. M. Gorbahn, U. Moldanazarova, K. H. Sieja, E. Stamou, M. Tabet, The anatomy of $K^+ \to \pi^+ \nu \bar{\nu}$ distributions. arXiv:2312.06494

13. F.-Z. Chen, Q. Wen, F. Xu, Correlating $B \to K^{(*)} \nu \bar{\nu}$ and flavor anomalies in SMEFT. arXiv:2401.11552

14. S. Bruggisser, L. Grabitz, S. Westhoff, Global analysis of the ALP effective theory. arXiv:2308.11703

15. T. Felkl, A. Giri, R. Mohanta, M.A. Schmidt, When energy goes missing: new physics in $b \to s \nu \nu$ with sterile neutrinos. Eur. Phys. J. C **83**, 12 1135 (2023). arXiv:2309.02940

16. A. Berezhnoy, D. Melikhov, $B \to K^* M_X$ vs $B \to K M_X$ as a probe of a scalar-mediator dark matter scenario. arXiv:2309.17191

17. W. Altmannshofer, A. Crivellin, H. Haigh, G. Inguglia, J. Martin Camalich, Light new physics in $B \to K^{(*)} \nu \bar{\nu}$? arXiv:2311.14629

18. K. Fridell, M. Ghosh, T. Okui, K. Tobioka, Decoding the $B \to K \nu \nu$ excess at Belle II: kinematics, operators, and masses. arXiv:2312.12507

19. D. McKeen, J.N. Ng, D. Tuckler, Higgs portal interpretation of the Belle II $B^+ \to K^+ \nu \nu$ measurement. arXiv:2312.00982

20. S.-Y. Ho, J. Kim, P. Ko, Recent $B^+ \to K^+ \nu \nu$ Excess and muon $g - 2$ illuminating light dark sector with Higgs portal. arXiv:2401.10112

21. D. Barducci, M. Fabbrichesi, E. Gabrielli, Neutral hadrons disappearing into the darkness. Phys. Rev. D **98**, 30 35049 (2018). arXiv:1806.05678

22. P. Fayet, On the search for a new spin 1 boson. Nucl. Phys. B **187**, 184–204 (1981)

23. L.B. Okun, Limits of electrodymanics: paraphotons? Sov. Phys. JETP **56**, 502 (1982)

24. H. Georgi, P.H. Ginsparg, S.L. Glashow, Photon oscillations and the cosmic background radiation. Nature **306**, 765–766 (1983)

25. B. Holdom, Two U(1)'s and epsilon charge shifts. Phys. Lett. B **166**, 196–198 (1986)

26. P. Fayet, Extra U(1)'s and new forces. Nucl. Phys. B **347**, 743–768 (1990)

27. J. Alexander et al., Dark Sectors 2016 Workshop: Community Report, 8 (2016). arXiv:1608.08632

28. M. Fabbrichesi, E. Gabrielli, G. Lanfranchi, The dark photon. arXiv:2005.01515

29. B.-A. Gradwohl, J.A. Frieman, Dark matter, long range forces, and large scale structure. Astrophys. J. **398**, 407–424 (1992)

30. E.D. Carlson, M.E. Machacek, L.J. Hall, Self-interacting dark matter. Astrophys. J. **398**, 43–52 (1992)

31. R. Foot, Mirror matter-type dark matter. Int. J. Mod. Phys. D **13**, 2161–2192 (2004). arxiv:astro-ph/0407623

32. L. Ackerman, M.R. Buckley, S.M. Carroll, M. Kamionkowski, Dark matter and dark radiation. Phys. Rev. D **79**, 023519 (2009). arXiv:0810.5126

33. J. Fan, A. Katz, L. Randall, M. Reece, Dark-disk universe. Phys. Rev. Lett. **110**, 21 211302 (2013). arXiv:1303.3271

34. R. Foot, S. Vagnozzi, Dissipative hidden sector dark matter. Phys. Rev. D **91**, 023512 (2015). arXiv:1409.7174

35. M. Heikinheimo, M. Raidal, C. Spethmann, H. Veermäe, Dark matter self-interactions via collisionless shocks in cluster mergers. Phys. Lett. B **749**, 236–241 (2015). arXiv:1504.04371

36. P. Agrawal, F.-Y. Cyr-Racine, L. Randall, J. Scholtz, Make dark matter charged again. JCAP **05**, 022 (2017). arXiv:1610.04611

37. J.T. Acuña, M. Fabbrichesi, P. Ullio, Phenomenological consequences of an interacting multicomponent dark sector. Phys. Rev. D **102**, 8 [arXiv:2005.04146]083009 (2020). arXiv:2005.04146

38. E. Gabrielli, M. Raidal, Exponentially spread dynamical Yukawa couplings from nonperturbative chiral symmetry breaking in the dark sector. Phys. Rev. D **89**, 1 015008 (2014). arXiv:1310.1090

39. E. Gabrielli, L. Marzola, M. Raidal, Radiative Yukawa couplings in the simplest left-right symmetric model. Phys. Rev. D **95**, 3 035005 (2017). arXiv:1611.00009

40. E. Gabrielli, M. Heikinheimo, B. Mele, M. Raidal, Dark photons and resonant monophoton signatures in Higgs boson decays at the LHC. Phys. Rev. D **90**, 5 055032 (2014). arXiv:1405.5196

41. S. Biswas, E. Gabrielli, M. Heikinheimo, B. Mele, Higgs-boson production in association with a dark photon in $e^+ e^-$ collisions. JHEP **06**, 102 (2015). arXiv:1503.05836

42. S. Biswas, E. Gabrielli, M. Heikinheimo, B. Mele, Dark-photon searches via Higgs-boson production at the LHC. Phys. Rev. D **93**, 9 093011 (2016). arXiv:1603.01377

43. S. Biswas, E. Gabrielli, M. Heikinheimo, B. Mele, Dark-photon searches via ZH production at e^+e^- colliders. Phys. Rev. D **96**, 5055012 (2017). arXiv:1703.00402

44. S. Biswas, E. Gabrielli, B. Mele, Dark photon searches via Higgs boson production at the LHC and beyond. Symmetry **14**, 81522 (2022). arXiv:2206.05297

45. H. Beauchesne, C.-W. Chiang, Observability of the Higgs boson decay to a photon and a dark photon. Phys. Rev. D **108**, 1 015018 (2023). arXiv:2304.04165

46. ATLAS Collaboration, G. Aad et al., Search for dark photons from Higgs boson decays via ZH production with a photon plus missing transverse momentum signature from pp collisions at $\sqrt{s} = 13$ TeV with the ATLAS detector. JHEP **07**, 133 (2023). arXiv:2212.09649

47. C.M.S. Collaboration, A.M. Sirunyan et al., Search for dark photons in Higgs boson production via vector boson fusion in proton–proton collisions at $\sqrt{s} = 13$ TeV. JHEP **03**, 011 (2021). arXiv:2009.14009

48. E. Gabrielli, B. Mele, M. Raidal, E. Venturini, FCNC decays of Standard Model fermions into a dark photon. Phys. Rev. D **94**, 11115013 (2016). arXiv:1607.05928

49. M. Fabbrichesi, E. Gabrielli, B. Mele, Hunting down massless dark photons in kaon physics. Phys. Rev. Lett. **119**, 3031801 (2017). arXiv:1705.03470

50. M. Fabbrichesi, E. Gabrielli, B. Mele, Z boson decay into light and darkness. Phys. Rev. Lett. **120**, 17171803 (2018). arXiv:1712.05412

51. A. Comelato, E. Gabrielli, Untangling the spin of a dark boson in Z decays. Phys. Rev. D **102**, 1 015028 (2020). arXiv:2006.00973

52. M. Cobal, C. De Dominicis, M. Fabbrichesi, E. Gabrielli, J. Magro, B. Mele, G. Panizzo, Z-boson decays into an invisible dark photon at the LHC, HL-LHC and future lepton colliders. Phys. Rev. D **102**(3), 035027 (2020). arXiv:2006.15945

53. B.A. Dobrescu, Massless gauge bosons other than the photon. Phys. Rev. Lett. **94**, 151802 (2005). arxiv:hep-ph/0411004

54. G. Isidori, Soft-photon corrections in multi-body meson decays. Eur. Phys. J. C **53**, 567–571 (2008). arXiv:0709.2439

55. A. Ali, P. Ball, L.T. Handoko, G. Hiller, A comparative study of the decays $B \to (K, K^*)\ell^+\ell^-$ in Standard Model and supersymmetric theories. Phys. Rev. D **61**, 074024 (2000). arxiv:hep-ph/9910221

56. C. Bobeth, G. Hiller, D. van Dyk, C. Wacker, The decay $B \to K\ell^+\ell^-$ at low hadronic recoil and model-independent $\Delta B = 1$ constraints. JHEP **01**, 107 (2012). arXiv:1111.2558

57. G. Buchalla, A.J. Buras, QCD corrections to rare K and B decays for arbitrary top quark mass. Nucl. Phys. B **400**, 225–239 (1993)

58. G. Buchalla, A.J. Buras, The rare decays $K \to \pi\nu\bar{\nu}$, $B \to X\nu\bar{\nu}$ and $B \to l^+l^-$: an update. Nucl. Phys. B **548**, 309–327 (1999). arxiv:hep-ph/9901288

59. M. Misiak, J. Urban, QCD corrections to FCNC decays mediated by Z penguins and W boxes. Phys. Lett. B **451**, 161–169 (1999). arxiv:hep-ph/9901278

60. J. Brod, M. Gorbahn, E. Stamou, Two-loop electroweak corrections for the $K \to \pi\nu\bar{\nu}$ decays. Phys. Rev. D **83**, 034030 (2011). arXiv:1009.0947

61. A. Sommerfeld, Über die Beugung und Bremsung der Elektronen. Annalen Phys. **403**(3), 257–330 (1931)

62. E. Fermi, An attempt of a theory of beta radiation. 1. Z. Phys. **88**, 161–177 (1934)

63. S. Weinberg, Infrared photons and gravitons. Phys. Rev. **140**, B516–B524 (1965)

64. E. Gabrielli, M. Palmiotto, Magnetic-dipole corrections to R_K and R_{K*} in the Standard Model and dark photon scenarios. JHEP **10**, 145 (2020). arXiv:1910.14385

65. BaBar Collaboration, J.P. Lees et al., Search for $B \to K^{(*)}\nu\bar{\nu}$ and invisible quarkonium decays. Phys. Rev. D **87**(11), 112005 (2013). arXiv:1303.7465

66. Belle Collaboration, J. Grygier et al., Search for $B \to h\nu\bar{\nu}$ decays with semileptonic tagging at Belle. Phys. Rev. D **96**(9), 091101 (2017). arXiv:1702.03224. [Addendum: Phys. Rev. D 97, 099902 (2018)]

67. Private communications with Belle collaboration

68. J. Martin Camalich, M. Pospelov, P.N.H. Vuong, R. Ziegler, J. Zupan, Quark flavor phenomenology of the QCD axion. Phys. Rev. D **102**(1), 015023 (2020). arXiv:2002.04623

69. M. Ciuchini, E. Gabrielli, G.F. Giudice, The chromomagnetic dipole operator and the B semileptonic branching ratio. Phys. Lett. B **388**, 353–365 (1996). arXiv:hep-ph/9604438. [Erratum: Phys. Lett. B 393, 489–490 (1997)]

70. P. Colangelo, F. De Fazio, R. Ferrandes, T.N. Pham, FCNC B_s and $Lambda_b$ transitions: Standard Model versus a single universal extra dimension scenario. Phys. Rev. D **77**, 055019 (2008). arXiv:0709.2817

71. DELPHI Collaboration, W. Adam et al., Study of rare b decays with the DELPHI detector at LEP. Z. Phys. C **72**, 207–220 (1996)

72. LHCb Collaboration, R. Aaij et al., Measurement of the ratio of branching fractions $BR(B_0 \to K^{\star 0}\gamma)/BR(B_{s0} \to \phi\gamma)$ and the direct CP asymmetry in $B_0 \to K^{\star 0}\gamma$. Nucl. Phys. B **867**, 1–18 (2013). arXiv:1209.0313

73. J. Lyon, R. Zwicky, Isospin asymmetries in $B \to (K^*, \rho)\gamma / l^+l^-$ and $B \to Kl^+l^-$ in and beyond the Standard Model. Phys. Rev. D **88**, 9 094004 (2013)

74. L. Li, M. Ruan, Y. Wang, Y. Wang, Analysis of $Bs \to \phi\nu\nu^-$ at CEPC. Phys. Rev. D **105**, 11114036 (2022). arXiv:2201.07374

75. Y. Amhis, M. Kenzie, M. Reboud, A.R. Wiederhold, Prospects for searches of $b \to s\nu\bar{\nu}$ decays at FCC-ee. JHEP **01**, 144 (2024). arXiv:2309.11353